

# Conformational and Noncovalent Complexation Changes in Proteins during Electrospray Ionization

Peter Nemes, Samita Goyal, and Akos Vertes\*

Department of Chemistry, W. M. Keck Institute for Proteomics Technology and Applications, George Washington University, Washington, D.C. 20052

Electrospray ion sources efficiently produce gas-phase ions from proteins and their noncovalent complexes. Charge-state distributions of these ions are increasingly used to gauge their conformations in the solution phase. Here we investigate how this correlation is affected by the spraying conditions at the early stage of droplet generation, prior to the ionization process. We followed the folding behavior of model proteins cytochrome *c* and ubiquitin and the dissociation of the noncovalent holo-myoglobin complex. Spray current measurements, fast Taylor cone imaging, and mass analysis of the generated ions indicated that the protein structure experienced conformational or complexation changes upon variations in the spraying mode of the electrospray ionization source. These effects resulted in a departure from the original secondary, tertiary, and quaternary structure of proteins, possibly introducing artifacts in related studies. Therefore, if a particular gas-phase ion conformation is required or correlations with the liquid-phase conformations are studied, it is advantageous to maintain a particular spraying mode. Alternatively, spraying mode-induced changes can be utilized to alter the structure of proteins in, for example, time-resolved experiments for the study of protein folding dynamics.

For an increasing number of biomolecules, electrospray ionization (ESI) is used for both the determination of their gas-phase ion structure<sup>1–5</sup> and by inference their folding and complexation in the solution phase.<sup>6–8</sup> In many investigations, ESI is believed to preserve the solution-phase protein structure and the composition of noncovalent complexes.<sup>9–11</sup> The three most relevant ESI-

based methodologies, charge-state distribution (CSD) analysis, amide hydrogen/deuterium-exchange experiments, and ion mobility studies, have provided a wealth of information on structural, dynamic, and conformational properties of proteins.<sup>7,8,12–16</sup> For example, ESI mass spectrometry (MS) probes the coexisting conformations of solution-phase proteins with high mass accuracy, superior sensitivity, and rapid detection. These unique features have enabled ESI-MS to complement conventional analytical and biophysical techniques, such as nuclear magnetic resonance (NMR), circular dichroism, Fourier transform infrared spectroscopy, tryptophan fluorescence, and scattering methods, used in protein research.

In these techniques, ESI transfers the solution-phase proteins as multiply charged quasi-molecular ions into the gas phase. Proteins electrosprayed from native-like conformations in solution retain their structures and yield narrow CSDs centered at higher *m/z* values, whereas those ionized under denaturing solution conditions give a wider charge-state envelope at higher ionic states (i.e., lower *m/z*).<sup>17–19</sup> These observations have been explained by the modified accessibility of ionizable basic sites, changes in their specific *pK<sub>a</sub>* values, and increase in the overall surface area of the protein.<sup>17–23</sup> Recent studies have also shown a nearly linear correlation between the surface area and the number of charges accommodated by the macromolecule,<sup>24,25</sup> for a wide range of protein sizes (kDa to MDa).<sup>25</sup>

\* To whom correspondence should be addressed. E-mail: vertes@gwu.edu.

- (1) Gidden, J.; Ferzoco, A.; Baker, E. S.; Bowers, M. T. *J. Am. Chem. Soc.* **2004**, *126*, 15132–15140.
- (2) Liu, D. F.; Wytttenbach, T.; Carpenter, C. J.; Bowers, M. T. *J. Am. Chem. Soc.* **2004**, *126*, 3261–3270.
- (3) Kaleta, D. T.; Jarrold, M. F. *J. Phys. Chem. A* **2002**, *106*, 9655–9664.
- (4) Hilderbrand, A. E.; Clemmer, D. E. *J. Phys. Chem. B* **2005**, *109*, 11802–11809.
- (5) Myung, S.; Fioroni, M.; Julian, R. R.; Koeniger, S. L.; Baik, M. H.; Clemmer, D. E. *J. Am. Chem. Soc.* **2006**, *128*, 10833–10839.
- (6) Eyles, S. J.; Kaltashov, I. A. *Methods* **2004**, *34*, 88–99.
- (7) Yan, X. G.; Watson, J.; Ho, P. S.; Deinzer, M. L. *Mol. Cell. Proteomics* **2004**, *3*, 10–23.
- (8) Maier, C. S.; Deinzer, M. L. In *Biological Mass Spectrometry*; Burlingame, A. L., Ed.; Methods in Enzymology 402, Elsevier Academic Press Inc.: San Diego, 2005; pp 312–360.
- (9) Bothner, B.; Suizdak, G. *ChemBioChem* **2004**, *5*, 258–260.

- (10) Ruotolo, B. T.; Giles, K.; Campuzano, I.; Sandercock, A. M.; Bateman, R. H.; Robinson, C. V. *Science* **2005**, *310*, 1658–1661.
- (11) Doerr, A. *Nat. Methods* **2006**, *3*, 72–73.
- (12) Loo, J. A. *Mass Spectrom. Rev.* **1997**, *16*, 1–23.
- (13) Smith, D. L.; Deng, Y. Z.; Zhang, Z. Q. *J. Mass Spectrom.* **1997**, *32*, 135–146.
- (14) Grandori, R. *Curr. Org. Chem.* **2003**, *7*, 1589–1603.
- (15) Koeniger, S. L.; Merenbloom, S. I.; Valentine, S. J.; Jarrold, M. F.; Udseth, H. R.; Smith, R. D.; Clemmer, D. E. *Anal. Chem.* **2006**, *78*, 4161–4174.
- (16) Merenbloom, S. I.; Koeniger, S. L.; Valentine, S. J.; Plasencia, M. D.; Clemmer, D. E. *Anal. Chem.* **2006**, *78*, 2802–2809.
- (17) Chowdhury, S. K.; Katta, V.; Chait, B. T. *J. Am. Chem. Soc.* **1990**, *112*, 9012–9013.
- (18) Katta, V.; Chait, B. T. *Rapid Commun. Mass Spectrom.* **1991**, *5*, 214–217.
- (19) Loo, J. A.; Loo, R. R. O.; Udseth, H. R.; Edmonds, C. G.; Smith, R. D. *Rapid Commun. Mass Spectrom.* **1991**, *5*, 101–105.
- (20) Katta, V.; Chait, B. T. *J. Am. Chem. Soc.* **1991**, *113*, 8534–8535.
- (21) Fenn, J. B. *J. Am. Chem. Soc. Mass Spectrom.* **1993**, *4*, 524–535.
- (22) Le Blanc, J. C. Y.; Beuchemin, D.; Siu, K. W. M.; Guevremont, R.; Berman, S. S. *Org. Mass Spectrom.* **1991**, *26*, 831–839.
- (23) Carbeck, J. D.; Severs, J. C.; Gao, J. M.; Wu, Q. Y.; Smith, R. D.; Whitesides, G. M. *J. Phys. Chem. B* **1998**, *102*, 10596–10601.
- (24) Hautreux, M.; Hue, N.; de KerDaniel, A. D.; Zahir, A.; Malec, V.; Laprevote, O. *Int. J. Mass Spectrom.* **2004**, *231*, 131–137.
- (25) Kaltashov, I. A.; Mohimen, A. *Anal. Chem.* **2005**, *77*, 5370–5379.

Based on the evidence accumulated in the literature, charge-state patterns are commonly accepted to be correlated with the higher-order structure of proteins.<sup>26,27</sup> Comparative studies on the dynamics of protein folding by ESI-MS and optical spectroscopic methods have revealed that the CSD is primarily sensitive to changes in the tertiary structure of the protein, whereas changes in the secondary structure have minor effects.<sup>28,29</sup> This correlation, however, is not necessarily valid in all cases.<sup>30–32</sup> The CSD strongly depends on the intrinsic properties of the protein such as its sequence, conformation,<sup>28,33</sup> and gas-phase chemistry.<sup>34–36</sup> In addition, various experimental conditions may also play a decisive role in the higher-order structure, including analyte concentration,<sup>37</sup> pH,<sup>17,28,29</sup> and composition<sup>17,19,27,38,39</sup> of the solvent, temperature,<sup>22,39–41</sup> redox reagents,<sup>22,42</sup> masking effects,<sup>36</sup> droplet evaporation rate,<sup>21</sup> emitter geometry,<sup>43,44</sup> and instrumental settings.<sup>45,46</sup> It is crucial to control and evaluate the effects of these parameters as they can induce a departure from the solution-phase structure.

Various studies have demonstrated that the understanding of ESI fundamentals is of primary importance. For example, the electrochemical reactions inherent to the nature of electrostatic spraying<sup>47</sup> have been found to alter the composition or the pH of the solution.<sup>48–51</sup> As a result, proteins, sensitive to changes in the experimental conditions, can denature.<sup>52</sup> A similar effect can be

expected to occur due to acidification,<sup>53,54</sup> solvent fractionation,<sup>55</sup> and solute concentration increase<sup>56</sup> of evaporating droplets moving downstream. A recent study has also called attention to the fragmentation of large macromolecular complexes resulting when the electrosprayed droplet is too small to enclose the analyte.<sup>57</sup> This effect becomes even more important with the increasing use of nanoflow electrosprays that are thought to generate 10–100 times smaller droplets than regular electrosprays.<sup>58</sup>

Electrostatic spraying is known to exhibit a variety of spraying regimes. These spraying modes were classified based on the fluid dynamic behavior of the liquid meniscus (dripping, burst, pulsating, astable, and cone-jet regimes)<sup>59–61</sup> and the temporal variation of the spray current (axial modes I, II, and III).<sup>62</sup> A direct link was established between the two taxonomies<sup>63</sup> that showed the equivalence of the burst and axial I mode, the pulsating and axial II regime, and the cone-jet and axial III mode.<sup>59,62,64</sup> It was demonstrated that the various spraying modes generated droplets of differing sizes<sup>59,60,65</sup> and yielded diverse ionization efficiencies.<sup>65,66</sup>

We have recently reported on how the transition between the pulsating and cone-jet modes affects the nature and composition of produced ions.<sup>65</sup> In this contribution, we explore how changes in the operating mode of the ESI source affect the ionization, charge-state distributions, and complexation of model proteins. These correlations are probed by a combination of spray current measurements, fast Taylor cone imaging, and mass analysis of the produced ions.

## EXPERIMENTAL SECTION

The experimental setup, shown in Figure 1, was described in full detail elsewhere.<sup>65</sup> Briefly, a home-built electrospray source equipped with a low-noise syringe pump (Physio 22, Harvard Apparatus, Holliston, MA) was used to spray various solutions through stainless steel emitters with 130- $\mu\text{m}$ -i.d. and 260- $\mu\text{m}$ -o.d. blunt tip (90531, Hamilton Co., Reno, NV) or with 100- $\mu\text{m}$ -i.d. and 320- $\mu\text{m}$ -o.d. tapered tip (TaperTip, New Objective, Woburn, MA). Stable high voltage was generated by a regulated power supply (PS350, Stanford Research Systems, Inc., Sunnyvale, CA) and was directly applied to the emitter. All metal parts of the liquid supply system were floated to avoid an external loop in the ESI circuit.<sup>52</sup> This assured that the observed effects were directly related to the transitions in the spraying modes.

The electrohydrodynamic behavior of the Taylor cone was imaged by a fast camera (QICAM, QImaging, Burnaby, BC,

- (26) Loo, J. A.; He, J. X.; Cody, W. L. *J. Am. Chem. Soc.* **1998**, *120*, 4542–4543.  
 (27) Iavarone, A. T.; Jurcen, J. C.; Williams, E. R. *J. Am. Soc. Mass Spectrom.* **2000**, *11*, 976–985.  
 (28) Konermann, L.; Douglas, D. J. *Biochemistry* **1997**, *36*, 12296–12302.  
 (29) Konermann, L.; Rosell, F. I.; Mauk, A. G.; Douglas, D. J. *Biochemistry* **1997**, *36*, 6448–6454.  
 (30) Chillier, X. F. D.; Monnier, A.; Bill, H.; Gulacar, F. O.; Buchs, A.; McLuckey, S. A.; Van Berkel, G. J. *Rapid Commun. Mass Spectrom.* **1996**, *10*, 299–304.  
 (31) Konermann, L.; Douglas, D. J. *J. Am. Soc. Mass Spectrom.* **1998**, *9*, 1248–1254.  
 (32) Mao, D. M.; Babu, K. R.; Chen, Y. L.; Douglas, D. J. *Anal. Chem.* **2003**, *75*, 1325–1330.  
 (33) Loo, J. A.; Edmonds, C. G.; Udseth, H. R.; Smith, R. D. *Anal. Chem.* **1990**, *62*, 693–698.  
 (34) Smith, R. D.; Loo, J. A.; Loo, R. R. O.; Busman, M.; Udseth, H. R. *Mass Spectrom. Rev.* **1991**, *10*, 359–451.  
 (35) Schnier, P. D.; Gross, D. S.; Williams, E. R. *J. Am. Soc. Mass Spectrom.* **1995**, *6*, 1086–1097.  
 (36) Gumerov, D. R.; Dobo, A.; Kaltashov, I. A. *Eur. J. Mass Spectrom.* **2002**, *8*, 123–129.  
 (37) Wang, G. D.; Cole, R. B. *Anal. Chem.* **1995**, *67*, 2892–2900.  
 (38) Konermann, L.; Douglas, D. J. *Rapid Commun. Mass Spectrom.* **1998**, *12*, 435–442.  
 (39) Li, J. W.; Taraszka, J. A.; Counterman, A. E.; Clemmer, D. E. *Int. J. Mass Spectrom.* **1999**, *187*, 37–47.  
 (40) Mirza, U. A.; Cohen, S. L.; Chait, B. T. *Anal. Chem.* **1993**, *65*, 1–6.  
 (41) Fligge, T. A.; Przybylski, M.; Quinn, J. P.; Marshall, A. G. *Eur. Mass Spectrom.* **1998**, *4*, 401–404.  
 (42) Zhao, C.; Wood, T. D.; Bruckenstein, S. *J. Am. Soc. Mass Spectrom.* **2005**, *16*, 409–416.  
 (43) Li, K. Y.; Tu, H. H.; Ray, A. K. *Langmuir* **2005**, *21*, 3786–3794.  
 (44) Ek, P.; Sjudahl, J.; Roeraade, J. *Rapid Commun. Mass Spectrom.* **2006**, *20*, 3176–3182.  
 (45) Loo, J. A.; Loo, R. R. O. *J. Am. Soc. Mass Spectrom.* **1995**, *6*, 1098–1104.  
 (46) Schmidt, A.; Bahr, U.; Karas, M. *Anal. Chem.* **2001**, *73*, 6040–6046.  
 (47) de la Mora, J. F.; Van Berkel, G. J.; Enke, C. G.; Cole, R. B.; Martinez-Sanchez, M.; Fenn, J. B. *J. Mass Spectrom.* **2000**, *35*, 939–952.  
 (48) Blades, A. T.; Ikononou, M. G.; Kebarle, P. *Anal. Chem.* **1991**, *63*, 2109–2114.  
 (49) Van Berkel, G. J.; McLuckey, S. A.; Glish, G. L. *Anal. Chem.* **1992**, *64*, 1586–1593.  
 (50) Van Berkel, G. J.; Zhou, F. M.; Aronson, J. T. *Int. J. Mass Spectrom. Ion Processes* **1997**, *162*, 55–67.  
 (51) Ochran, R. A.; Konermann, L. *J. Am. Chem. Soc.* **2004**, *126*, 1748–1754.

- (52) Konermann, L.; Silva, E. A.; Sogbein, O. F. *Anal. Chem.* **2001**, *73*, 4836–4844.  
 (53) Zhou, S. L.; Edwards, A. G.; Cook, K. D.; Van Berkel, G. J. *Anal. Chem.* **1999**, *71*, 769–776.  
 (54) Zhou, S.; Prebyl, B. S.; Cook, K. D. *Anal. Chem.* **2002**, *74*, 4885–4888.  
 (55) Zhou, S. L.; Cook, K. D. *Anal. Chem.* **2000**, *72*, 963–969.  
 (56) Wortmann, A.; Kistler-Momotova, A.; Zenobi, R.; Heine, M. C.; Wilhelm, O.; Pratsinis, S. E. *J. Am. Soc. Mass Spectrom.* **2007**, *18*, 385–393.  
 (57) Hogan, C. J.; Kettleton, E. M.; Ramaswami, B.; Chen, D. R.; Biswas, P. *Anal. Chem.* **2006**, *78*, 844–852.  
 (58) Wilm, M.; Mann, M. *Anal. Chem.* **1996**, *68*, 1–8.  
 (59) Cloupeau, M.; Prunet-Foch, B. *J. Aerosol Sci.* **1994**, *25*, 1021–1036.  
 (60) Cloupeau, M.; Prunet-Foch, B. *J. Electrostatics* **1990**, *25*, 165–184.  
 (61) Marginean, I.; Nemes, P.; Vertes, A. *Phys. Rev. E* **2007**, *76*, 026320.  
 (62) Juraschek, R.; Rollgen, F. W. *Int. J. Mass Spectrom.* **1998**, *177*, 1–15.  
 (63) Marginean, I.; Parvin, L.; Heffernan, L.; Vertes, A. *Anal. Chem.* **2004**, *76*, 4202–4207.  
 (64) Marginean, I.; Nemes, P.; Vertes, A. *Phys. Rev. Lett.* **2006**, *97*, 064502.  
 (65) Nemes, P.; Marginean, I.; Vertes, A. *Anal. Chem.* **2007**, *79*, 3105–3116.  
 (66) Valaskovic, G. A.; Murphy, I. J. P.; Lee, M. S. *J. Am. Soc. Mass Spectrom.* **2004**, *15*, 1201–1215.

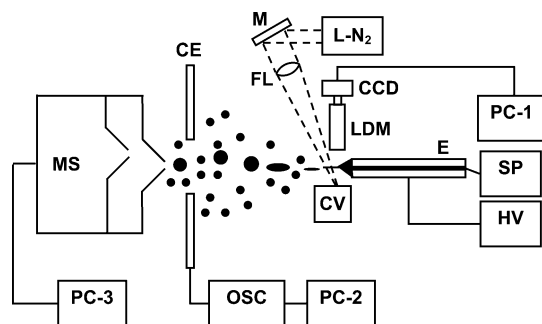


**Figure 1.** Schematics of experimental setup for electrohydrodynamic and chemical characterization of electrosprays: emitter (E), syringe pump (SP), high voltage power supply (HV), nitrogen laser (L-N<sub>2</sub>), mirror (M), focusing lens (FL), cuvette (CV), CCD camera (CCD) with long-distance microscope (LDM), personal computer (PC-1), counter electrode (CE), digital oscilloscope (OSC) with personal computer (PC-2), and mass spectrometer (MS) with personal computer (PC-3).

Canada) equipped with a long-distance microscope (KC, Infinity Photo-Optical Co., Boulder, CO). The liquid meniscus was stroboscopically back-illuminated with a pulsed light source. The illumination was achieved by utilizing the fluorescent emission from a laser dye solution (Coumarin 540A, Exciton, Dayton, OH) upon excitation with a 337.1-nm nitrogen laser (VSL-337, Newport Corp., Irvine, CA). A flat polished stainless steel plate (38.1 mm × 38.1 mm × 0.6 mm) was placed perpendicularly to the axis of the emitter at a distance of 10 mm from its tip. The spray current was measured on this counter electrode with a 500-MHz digital oscilloscope (WaveSurfer 452, LeCroy, Chestnut Ridge, NY) at a 25-kHz sampling rate. The counter electrode had a 6.0-mm-diameter circular opening in the center and was positioned in line with the center of the mass spectrometer inlet orifice by using an *x*-*y*-*z* mechanical translation stage (F38182 and NT37-979, Edmund Industrial Optics, Barrington, NJ). This arrangement allowed us to simultaneously analyze the spray current on the counter electrode and determine the nature and yield of the produced gas-phase ions by a mass spectrometer (JMS-T100LC AccuTOF mass spectrometer, JEOL Ltd., Peabody, MA). The orifice of the sampling cone was on axis with the electrospray emitter at a 12-mm distance from its tip. The ion-transfer optics of the mass spectrometer was adjusted for optimum signal intensity and resolution for each chemical species. Mass analysis was performed in positive ion mode for the *m/z* range of 100–4000. Each mass spectrum was acquired with an integration time of 2 s and averaged over 30 s. Data acquisition and processing was performed with the MassCenter software (Version 1.3.0, JEOL Ltd.).

Special care was taken to shield the spray assembly using a Faraday cage and a plastic enclosure to minimize the interferences by external electromagnetic fields and air currents, respectively. The electrospray system was allowed to stabilize every time (typically for 1 min) after adjusting the spray conditions (e.g., high voltage) to ensure that the proteins adopted a stable conformation before mass spectra were acquired. For example, refolding of denatured cytochrome *c* requires less than 10 s.<sup>67</sup> The electro-

sprayed protein solutions were kept at room temperature prior to analysis. To avoid changing the ionization and ion transmission conditions, the potentials on the ion optics and the temperature of the sampling cone were kept constant during experiments.

**Chemicals.** Ultrapure water (18.3 MΩ × cm) was produced using a deionization system (E-pure D4631, Barnstead, Dubuque, IA). Bovine heart cytochrome *c*, ubiquitin from bovine erythrocytes and myoglobin from equine heart were purchased from Sigma-Aldrich and were used as received to prepare 100 μM protein stock solutions with deionized water. The protein solutions were then diluted to a 10 μM final concentration with aqueous methanol (HPLC grade, Sigma-Aldrich) solvents also containing 1.5 mM sodium acetate (S209-500, Fischer Scientific) or glacial acetic acid (TraceSelect grade, Sigma-Aldrich) to obtain pH 3.75 ± 0.01. The pH values of the solvents were determined with a glass combination electrode (S90528, Fischer Scientific).

## RESULTS AND DISCUSSION

Depending on the experimental conditions (flow rate, spray voltage, solution conductivity, emitter geometry, etc.), electrostatic spraying can operate in a variety of spraying modes. In principle, it is possible to select a spraying mode by adjusting any of these variables. In practice, however, the spray voltage and the flow rate are the most easy to adjust. In the experiments reported here, only the spray voltage was varied to establish a given spraying mode.

The axial spraying regimes can be distinguished by monitoring the spray current on a counter electrode and by capturing the shape changes of the meniscus. This is shown in Figure 2 for a 10 μM cytochrome *c* solution prepared with 50% (v/v) ethanol that was acidified with acetic acid to pH 3.75. At 2500 V spray voltage and 1.0 μL/min flow rate, the spray showed a stable behavior;<sup>61</sup> i.e., the pulsating and the cone-jet modes alternated in time. Figure 2A shows the cone-jet to pulsating mode transition in the current measurement. In the cone-jet mode, the spray current had no appreciable ac component; only low-amplitude ~2-Hz electronic noise from the mass spectrometer was superimposed on the signal. The imaging experiments confirmed the formation of a steady-state Taylor cone, shown in Figure 2B. As the spray switched to the pulsating mode, the dc component of the spray current decreased by ~50 nA, and an ac component of 2.4 kHz frequency emerged. The pulsating meniscus exhibited jet ejection with characteristic kink-type instabilities (see in Figure 2B), followed by the production of larger primary droplets stemming from the relaxing liquid spindle.<sup>65</sup>

Of the various axial spraying regimes, the pulsating and cone-jet modes are the most suitable for the production of gas-phase ions.<sup>65,66</sup> To examine whether the spraying mode influenced the folding of the produced protein ions, we studied the CSDs of cytochrome *c*, ubiquitin, and myoglobin. These proteins were electrosprayed as 10 μM aqueous solutions prepared with 30–70% (v/v) methanol or ethanol at 10% alcohol increments. The pH values of the solutions were adjusted to 3.75 with acetic acid. The produced ions were mass analyzed while the spray voltage was gradually increased from the onset of the pulsating mode through the transition to the cone-jet mode up to its stability limit. For each solution composition and emitter voltage, the CSDs of the proteins were normalized for the same total area to yield the extracted mass spectra. This allowed us to deconvolute the CSDs

(67) Konermann, L.; Collings, B. A.; Douglas, D. J. *Biochemistry* **1997**, *36*, 5554–5559.

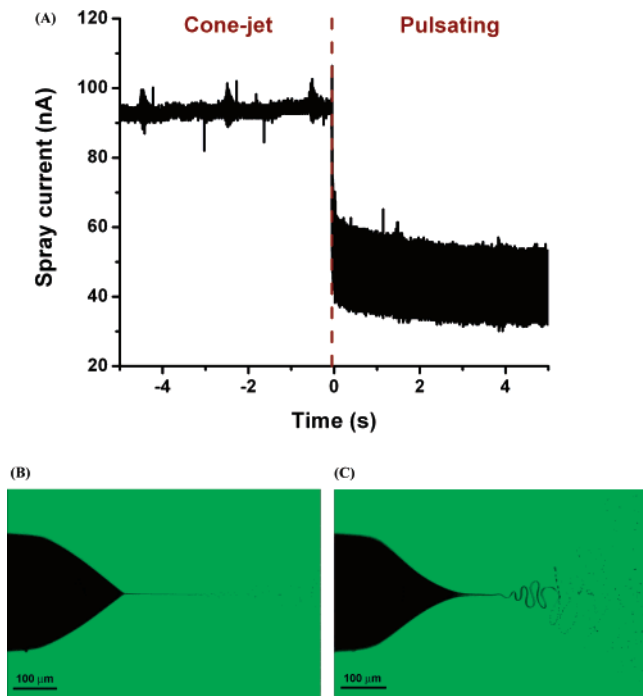


**Figure 2.** (A) Switching of spraying mode in astable regime reflected by spray current measurement for 10  $\mu\text{M}$  cytochrome *c* solution (50% ethanol, pH 3.75) sprayed at constant voltage (2500 V) and flow rate (1.0  $\mu\text{L}/\text{min}$ ). The cone-jet and pulsating modes were alternating in time at random. The cone-jet mode showed a spray current with high dc component (95 nA) and no appreciable ac component, whereas the pulsating regime exhibited a spray current with a lower dc component (42 nA) and an ac component with a pulsation frequency of 2.4 kHz. The established spraying mode was also confirmed by visualizing the electrohydrodynamic behavior of the meniscus. Images B and C show the Taylor cones typically observed in the cone-jet and pulsating modes, respectively.

by constrained fitting of the mass spectra with multiple Gaussians and to directly compare the CSDs acquired under different experimental conditions (spray voltage and regime). Unless otherwise mentioned, abundances for each protein conformer were represented by the area of the corresponding Gaussian curve.

**Two-State Protein: Cytochrome *c*.** The unfolding transition of cytochrome *c* is known to be highly cooperative between only two states: native and unfolded.<sup>28,38,68</sup> Similar to previous observations,<sup>14</sup> with increasing methanol or ethanol concentrations, the charge-state envelope of the cytochrome *c* underwent a dramatic change (data not shown). At low organic content, a single CSD was formed with a maximum at  $\text{Cyt}^{9+}$  corresponding to the native (N) conformation of the protein. Under slightly denaturing conditions ( $\sim 50\%$  alcohol), a second distribution emerged with a center,  $\nu_c$ , at 13+ that had been attributed to the unfolded state (U) of the cytochrome *c*. Above  $\sim 60\%$  (v/v) ethanol concentration, only the unfolded conformer was present.

A systematic comparison of the mass spectra acquired in pulsating and cone-jet modes revealed dramatic differences in the ionization efficiencies and in the appearance of the CSD envelopes. This effect was the most pronounced when both the folded and the unfolded states were populated. Shown in Figure 3 is the total ion chromatogram and the selected ion signal of the  $\text{Cyt}^{13+}$  species

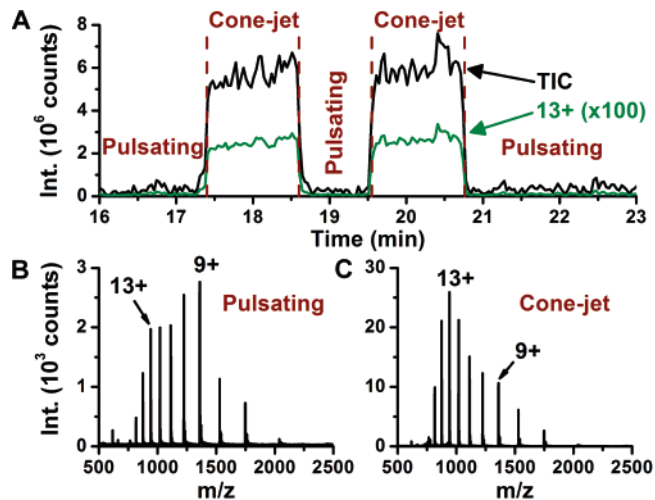


**Figure 3.** (A) Total ion current (TIC) and mass-selected ion chromatogram (100 times amplified) for charge state 13+ of cytochrome *c* at constant spray voltage and flow rate (50% ethanol, pH 3.75, other experimental conditions described in caption of Figure 2). Vertical dashed lines indicate the switching points between pulsating and cone-jet spraying modes alternating in time. Mass spectra averaged over (B) the pulsating, and (C) the cone-jet mode show an order of magnitude higher protein ion current in the cone-jet mode. Switching to cone-jet mode gave rise to a shift in the CSD with a maximum at 13+ (9+ diminished) that indicated the unfolding of the protein.

acquired under astable spraying mode conditions (50% ethanol and pH 3.75 at constant high voltage and flow rate).<sup>61</sup> Upon a spray mode change from the pulsating to the cone-jet regime, at least 1 order of magnitude enhancement was detected in the macromolecule ion current. Previous studies had shown similar behavior for small organic molecules<sup>65</sup> and small polypeptides.<sup>66</sup> Our current measurements indicated that higher ion yields prevailed for the cone-jet mode over a broad range of  $m/z$ .

Once the electrospray stabilized after the spraying mode change, the mass spectra averaged in the pulsating and the cone-jet modes (see Figure 3) revealed a significant difference between the CSDs. Time-resolved ESI-MS studies determined the folding time frame of cytochrome *c* to be within  $\sim 10$  s.<sup>67</sup> As the electrospray system was allowed to stabilize for 1 min after each spraying mode change, the cytochrome *c* folding had concluded before data acquisition took place. In the pulsating regime, the protein was mostly present in its native state ( $\nu_c = 9+$ ), whereas in the cone-jet mode, the unfolded structure was favored ( $\nu_c = 13+$ ). These shifts were observed to take place at  $\sim 1$ – $5$ -min irregular intervals, i.e., each time the spraying mode changed (see the ion chromatogram in Figure 3). As all the experimental conditions (flow rate, spray voltage, etc.) were held constant, the data collected in the astable spraying mode demonstrated that the CSD changes were solely induced by switching between the spraying modes.

The unfolding/refolding behavior was monitored over an extended range of spray voltages. These results can be seen in Figure 4, where the relative area of the native conformation (the area for the native state divided by the sum of the areas for the native and unfolded states,  $A_N$  and  $A_U$ , respectively) is depicted. As shown in inset A, throughout the pulsating regime the native

(68) Creighton, T. E. *Biochem. J.* **1990**, *270*, 1–16.

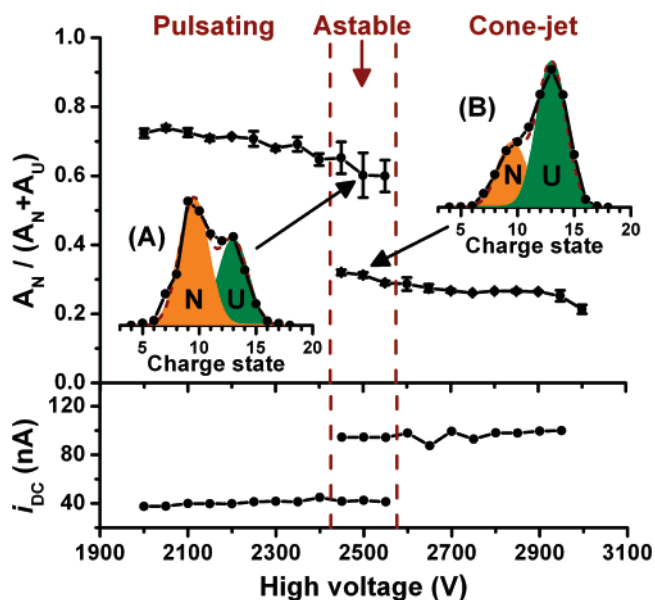


**Figure 4.** Unfolding of cytochrome *c* upon switching of ESI source spraying regime from pulsating to cone-jet mode. The relative area of the native conformer CSD,  $A_N/(A_N + A_U)$ , ( $A_N$  and  $A_U$  indicate the areas of the native and unfolded protein CSDs, respectively) and the dc component of the spray current ( $i_{DC}$ ) are depicted as a function of spray voltage. Error bars indicate the standard deviations of three measurements and are within symbols. Vertical dashed lines show the boundaries between the established axial spraying modes. Within the pulsating and the cone-jet regimes, the relative area of the native conformer CSD changes very little. In the astable region, where only the spraying regime is alternating in time (at constant spray voltage and flow rate), the CSDs observed in the pulsating (see inset A) and in the cone-jet (see inset B) modes show that the protein undergoes conformational changes. The higher spray current measured in the cone-jet mode suggests increased oxidation of the solvent converting water to protons. The resulting lower pH in the cone-jet mode can account for the unfolding of the protein.

form of the protein is more abundant. As the astable region was reached at 2450 V, the CSDs began to flip-flop in sync with the spraying mode alternating between the pulsating and cone-jet regimes. Thus, in this region, for every spray voltage the conformations were represented by two data points on the vertical axis. Upon further increasing the spray voltage (2600 V), the electrospray stabilized in the cone-jet mode, the unfolded conformer of cytochrome *c* became dominant, and the relative area of the native state significantly decreased.

Remarkably,  $A_N/(A_N + A_U)$ , and thus the CSD, as a function of spray voltage, remained essentially unchanged within the pulsating and cone-jet spraying regimes. For example, the mass spectra observed at the low- and high-stability limit of the pulsating regime (2000 and 2550 V, respectively) appeared to be very similar. Similarly, the mass spectra recorded at the boundaries of the cone-jet regime (2450 and 3000 V) were close to indistinguishable. This indicated that similar ionization conditions were met within a spraying regime, which provided robust conformer ion production with little sensitivity to voltage variations.

Several effects need to be considered to explain how cytochrome *c* ions undergo conformational changes when the spraying mode is altered. It is known that changes in the spraying mode are capable of inducing the reduction or oxidation of the

analyte and probably affect the pH of the solution.<sup>65</sup> Assuming that all the charge-balancing current is supplied by the oxidation of water,  $2H_2O \rightarrow 4H^+ + O_2 + 4e^-$ , using Faraday's law one obtains the electrolytically produced proton concentration as  $[H^+]_{elec} = i_{ES}/nFv_f$ , where  $i_{ES}$  is the electrospray current,  $n$  is the number of electrons transferred to produce an ion (for protons  $n = 1$ ),  $F$  is the Faraday constant, and  $v_f$  is the rate of solution supply.<sup>50</sup> Fluorescence measurements show that the pH directly calculated from the spray current is in good agreement with values determined by spectroscopic methods.<sup>53</sup> Thus, an upper limit for the pH shift upon spraying mode changes can be estimated.

Under the astable spraying conditions, e.g., at 2500 V emitter potential, the dc component of the measured spray current,  $i_{DC}$ , in the pulsating and cone-jet modes was 42 and 95 nA, respectively (see Figure 2A). For low buffer capacity solutions, at the applied flow rate (1.0  $\mu\text{L}/\text{min}$ ) and the measured  $i_{DC}$  the pH of the solution is calculated to decrease from the original 3.75 to 1.58 and 1.23 in pulsating and cone-jet modes, respectively. Thus, upon regime change to cone-jet mode, a pH change of 0.35 unit is expected that corresponds to an increase in the electrochemically produced proton concentration,  $[H^+]_{elec}$ , by a factor of  $\sim 2.3$ . According to literature data, this 0.35 unit pH change can account for the unfolding of cytochrome *c* in aqueous solutions.<sup>17,69</sup> Furthermore, these results are consistent with the acid-induced unfolding of cytochrome *c* at various alcohol concentrations.<sup>28</sup> Due to solvent evaporation from the droplets, further pH changes are known to occur downstream in the electrospray plume.<sup>54</sup> These changes can be similar in magnitude and due to differences in droplet size distributions might also depend on spraying modes.

The role of the spraying mode-induced pH change in the altered conformation of cytochrome *c* was probed by introducing a buffer. Mass spectra of the unbuffered and buffered protein solutions acquired under identical experimental conditions in the pulsating and the cone-jet modes are shown in Figure 5. As discussed above, in the unbuffered solution, the protein exhibited different conformations when ionized using the two spraying modes (Figure 5A versus Figure 5B). In the presence of a buffer, however, no change was observed in the CSDs produced in the two axial regimes (Figure 5C versus Figure 5D). These results underlined that the observed CSD changes were caused by the different pH shifts as the operating mode alternated between the pulsating and cone-jet modes.

**Multistate Protein: Ubiquitin.** The effects of spraying regime changes on CSDs observed for cytochrome *c* were also explored for ubiquitin (see Supporting Figure 1 in the Supporting Information). From 10  $\mu\text{M}$  solutions with low organic content ( $<40\%$ ), ubiquitin was ionized in its native conformation. The mass spectrum appeared to be composed of a single distribution of charge states peaking at 6+. Increasing the methanol concentration gave a gradual rise to several higher charge states. In contrast to the highly cooperative behavior of cytochrome *c*, this indicated that in addition to the native and unfolded states other conformations were also populated. Previous work based on NMR and MS utilizing hydrogen–deuterium exchange and CSD studies also

(69) Samalikova, M.; Matecko, I.; Muller, N.; Grandori, R. *Anal. Bioanal. Chem.* **2004**, *378*, 1112–1123.

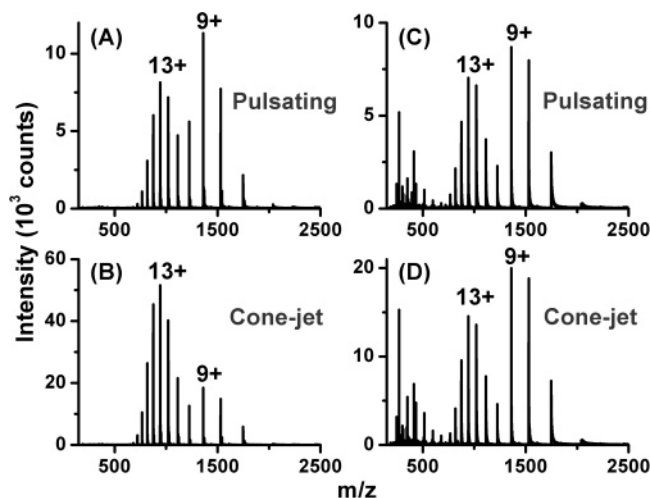


**Figure 5.** Effect of spraying mode on CSDs of 10  $\mu\text{M}$  cytochrome *c* solution in 50% ethanol for buffered and unbuffered solutions. For low buffer capacity solutions acidified with acetic acid (pH 3.75), the protein underwent conformational changes when the ESI source switched from (A) the pulsating to (B) the cone-jet mode. However, when electrospayed from a solution containing 1.5 mM sodium acetate buffer (pH 3.75) no shifts in the charge-state envelope were observed upon changing the spraying mode from (C) the pulsating to (D) the cone-jet mode. The two measurements were carried out at 2.0  $\mu\text{L}/\text{min}$  flow rate with the pulsating and cone-jet regimes maintained at 2700 and 3100 V, respectively. These results indicated that the unfolding of cytochrome *c* was due to the decreased pH in cone-jet mode (see text).

found that at low-salt and pH conditions a partially structured nonnative state (A-state) of ubiquitin became populated when the alcohol level exceeded  $\sim 40\%$ .<sup>70–72</sup>

When the ubiquitin solution was electrospayed in pulsating and cone-jet modes, a significant difference was noticed in the charge-state envelopes. At 3.75 pH, this effect was the most noticeable for solutions prepared with 60% (v/v) methanol, which was consistent with earlier results showing that these conditions favored the A-state.<sup>70–72</sup> The overlapping charge-state distributions of the N, A, and U conformers can be unraveled by chemometric tools, such as singular value decomposition or multivariate curve resolution-alternating least-squares methods.<sup>71,73</sup> The purpose of the present study, however, was to demonstrate the effect of spraying regime changes on the CSDs of proteins. Therefore, the CSDs of the individual conformer states were not deconvoluted. Instead, the abundance ratios of characteristic charge states were tracked to gauge the presence of various folding states.

Similarly to the case of cytochrome *c*, the mass spectra of ubiquitin acquired in pulsating and cone-jet modes (see the bottom panels in Figure 6) showed natively and denaturing ionization, respectively. For example, from the onset of the spray in the pulsating regime at 2200 V until 2650 V the base peak of the mass spectrum corresponded to the 6+ charge state. As the spray changed to cone-jet mode, however, the protein adopted a rather

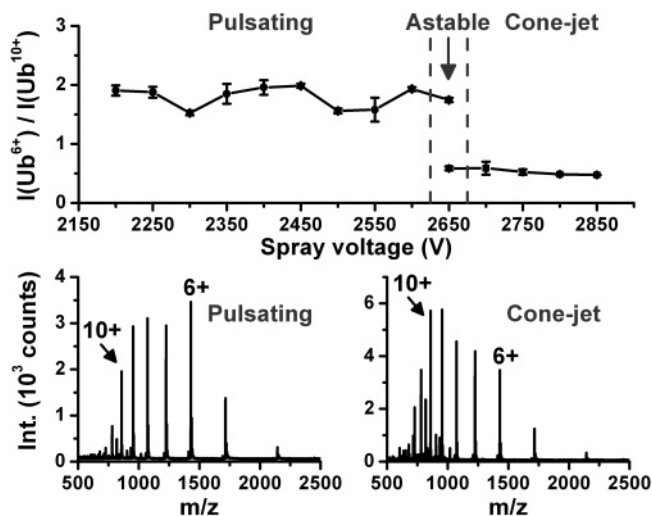


**Figure 6.** Unfolding of ubiquitin in 60% methanol caused by switching between pulsating and cone-jet modes. Upon the switch to cone-jet regime, the CSD of ubiquitin shifted to lower  $m/z$  values. This shift was induced by applying higher spray voltages and monitored by following the abundance ratio of the charge states 6+ and 10+ that corresponded to the native and an unfolded state, respectively. The vertical dashed lines show boundaries between the established spraying regimes. Error bars indicate the standard deviations of three measurements. In the astable region, at 2  $\mu\text{L}/\text{min}$  constant flow rate and 2650 V spray voltage, the mass spectrum acquired in pulsating regime showed that the protein was ionized mostly in its native conformer (base peak was at 6+ state). However, when sprayed in the cone-jet mode, a shift to the 10+ (and 9+) charge states indicated that the majority of the ubiquitin was present in an unfolded conformation. Similar to the case of cytochrome *c*, these effects could be explained by the enhanced acidification of the solution in cone-jet mode.

unfolded state with a base peak at the 10+ charge state. By following the ratio of the native 6+ and the less structured 10+ state abundances,  $I(\text{Ub}^{6+})/I(\text{Ub}^{10+})$ , as a function of the spray voltage (see top panel in Figure 6), we found that the dynamic change in the protein structure was linked to the spraying mode only and was not affected by the high voltage. As expressed by a nearly constant  $I(\text{Ub}^{6+})/I(\text{Ub}^{10+})$  ratio in the figure, throughout both the pulsating and the cone-jet regimes, the tertiary structure of the ubiquitin remained unchanged. At 2650 V emitter potential, when the astable regime was reached, however, the protein CSD envelope was alternating in time. This provided us with further evidence that the unfolding of the ubiquitin was linked to the spraying mode changes only and not to the altered experimental conditions. The unfolding of ubiquitin, similarly to that of cytochrome *c*, can be explained by spraying regime-induced pH changes in the electrospayed solution.

**Noncovalent Complexation: Myoglobin.** Unlike in cytochrome *c*, in holomyoglobin, the heme prosthetic group is retained inside a hydrophobic pocket through noncovalent interactions. The hydrophobicity of the heme moiety prevents the dissociation of this complex, so in the absence of an organic phase in moderately acidic solutions ( $2.6 < \text{pH} < 3.5$ ), it remains intact.<sup>74</sup> Electrospayed at pH 3.75 from solutions containing less than  $\sim 10\%$  (v/v) methanol, the myoglobin produced intact ions with

(70) Brutscher, B.; Bruschiweiler, R.; Ernst, R. R. *Biochemistry* **1997**, *36*, 13043–13053.

(71) Mohimen, A.; Dobo, A.; Hoerner, J. K.; Kaltashov, I. A. *Anal. Chem.* **2003**, *75*, 4139–4147.

(72) Hoerner, J. K.; Xiao, H.; Kaltashov, I. A. *Biochemistry* **2005**, *44*, 11286–11294.

(73) Navea, S.; Tauler, R.; de Juan, A. *Anal. Chem.* **2006**, *78*, 4768–4778.

(74) Sage, J. T.; Morikis, D.; Champion, P. M. *Biochemistry* **1991**, *30*, 1227–1237.

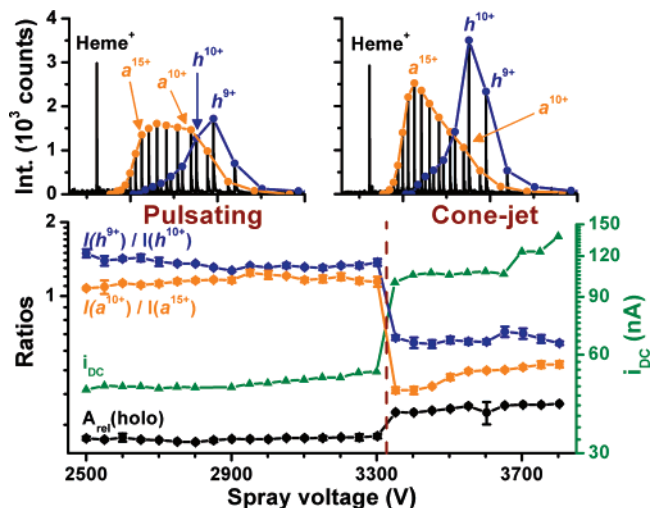


**Figure 7.** Effect of spraying regime changes on the integrity and conformation of the noncovalent myoglobin complex. A solution of 10  $\mu\text{M}$  myoglobin in 30% methanol (pH 3.75) was electrosprayed at 1  $\mu\text{L}/\text{min}$  flow rate using a microelectrospray source (New Objective emitter). The mass spectra in the insets show the CSDs for the intact holomyoglobin ( $h^{n+}$ ), and its dissociation products the apomyoglobin ( $a^{m+}$ ) and the heme prosthetic group (Heme $^{+}$ ). Dissociation of the myoglobin is reported by the relative area of the holo form ( $A_{\text{rel}}(\text{holo}) = \sum I(h^{n+}) / (\sum I(h^{n+}) + \sum I(a^{m+}) + I(\text{Heme}^{+}))$ ) as a function of spray voltage (black filled circles), where  $I$  stands for the ionic abundance in the mass spectrum,  $h^{n+}$  is  $[\text{holomyoglobin} + n\text{H}]^{n+}$ , and  $a^{m+}$  is  $[\text{apomyoglobin} + m\text{H}]^{m+}$  and  $n, m$  indicate the charge states. The unfolding of the holo and apo specimens is presented by the ratios  $I(h^{9+})/I(h^{10+})$  and  $I(a^{10+})/I(a^{15+})$  shown in royal blue and orange filled circles, respectively. Error bars indicate the standard deviations of three measurements and are within symbols. The vertical dashed line separates the two spraying regimes. As the operating mode switches from the pulsating to the cone-jet mode, also indicated by a jump in the dc component of the spray current,  $i_{\text{dc}}$ , at 3350 V, reduced  $h^{9+}/h^{10+}$  and  $a^{10+}/a^{15+}$  ratios are obtained. This indicates the unfolding of both species. Concurrently,  $A_{\text{rel}}(\text{holo})$  increases, showing that softer ionization conditions are achieved, i.e., the integrity of the noncovalent complex is preserved to a higher degree in the cone-jet regime.

the CSD centered around the 9+ state. Above  $\sim 20\%$  organic solvent content, the formation of the apoprotein was also observed along with a wide distribution of charge states. This can be seen in the mass spectrum of 10  $\mu\text{M}$  myoglobin solution at pH 3.75 prepared with 30% methanol (see the insets in Figure 7). The CSD of the intact holomyoglobin ( $h^{n+}$ ) followed a unimodal distribution centered on the  $h^{9+}$  species, corresponding to the native conformation. Dissociation of the noncovalent complex resulted in the formation of the Heme $^{+}$  ion and in a wide apomyoglobin CSD ( $a^{m+}$ ) ranging from  $a^{6+}$  to  $a^{20+}$ .

By changing the spray voltage, we found that the extent of the holomyoglobin dissociation and the CSD of the apoprotein depended on the established spraying mode. The individual conformations were not deconvoluted in the data analysis. Instead, the integrity of the heme protein was monitored by the relative area of the holo form,  $A_{\text{rel}}(\text{holo})$ , expressed as  $\sum I(h^{n+}) / (\sum I(h^{n+}) + \sum I(a^{m+}) + I(\text{Heme}^{+}))$ , where  $I$  represented the ion abundances. The conformations of the holo- and apomyoglobin were characterized by the  $I(h^{9+})/I(h^{10+})$  and  $I(a^{10+})/I(a^{15+})$  ratios, respectively.

At 1  $\mu\text{L}/\text{min}$  flow rate and low voltages (2500–3300 V), the spray operated in the pulsating mode. Within this regime, applying higher voltages did not appreciably affect the conformation of the

holo and apo forms (see the unchanged  $I(h^{9+})/I(h^{10+})$  and  $I(a^{10+})/I(a^{15+})$  ratios in Figure 7) and produced the same type of ions over an  $\sim 800\text{-V}$  range. As the emitter potential was increased from 3300 to 3350 V, the Taylor cone pulsation ceased and the dc component of the spray current significantly increased, indicating that the operating mode switched to the cone-jet regime (see  $i_{\text{dc}}$  in Figure 7). Concurrently,  $A_{\text{rel}}(\text{holo})$  increased, indicating less dissociation of the myoglobin, i.e., “milder” ionization conditions in the cone-jet regime. Upon the pulsating to cone-jet mode transition, the  $I(h^{9+})/I(h^{10+})$  and  $I(a^{10+})/I(a^{15+})$  ratios took lower values. This showed enrichment in the highly unfolded protein conformations (appearing at lower  $m/z$  values) for the holo and apo species. These ratios remained constant throughout the cone-jet regime over a range of 450 V. Thus, the ionization conditions appeared unaffected by the increasing spray voltage and were determined by the spraying mode only. In the pulsating mode, the base peak corresponded to the  $h^{9+}$  species (see Figure 7). As the electrospray switched to the cone-jet regime, the CSDs of both the holo- and the apoprotein gradually shifted to smaller  $m/z$  values, with the maximum for the apo species ultimately approaching 15+ (see the insets in Figure 7). The low cooperativity in the unfolding behavior of the apomyoglobin—compared to that of cytochrome  $c$ —indicated that multiple conformers were involved in the process. Previous investigations of this transition under similar experimental conditions using NMR and optical spectroscopy,<sup>75</sup> calorimetric,<sup>76,77</sup> and ESI-MS<sup>38,71,78</sup> methods arrived at similar conclusions.

As discussed in detail for the case of cytochrome  $c$ , the shift in the apomyoglobin CSD upon spraying regime change could be rationalized by considering local changes in the pH at the emitter. As the spray switched to the cone-jet mode and the solution became more acidic due to the enhanced oxidation of water, the equilibrium between the coexisting native (N), intermediate (I), extended (E), and unfolded (U) conformers<sup>79</sup> was shifted toward the more unfolded states. Earlier chemometric studies over the 2.5–10 pH range revealed that the CSDs of these conformational isomers were centered on the  $\nu_{\text{N}} = 8.9$ ,  $\nu_{\text{I}} = 10.4$ ,  $\nu_{\text{E}} = 15.3$ , and  $\nu_{\text{U}} = 20.5$  charge states, respectively.<sup>71,78</sup> The mass spectra of myoglobin shown in these studies (e.g., Figure 1 in ref 78) were very similar to ours, allowing us to directly compare the CSDs. In light of the deconvoluted CSD data in ref 78, the CSD changes observed in the pulsating to cone-jet transition were consistent with a related change in conformation between the intermediate and extended states.

Considering the enhanced acidification of the solution in the cone-jet mode, also indicated by the unfolding of the apoprotein, it seems counterintuitive that the noncovalent interaction in myoglobin is preserved to a better extent in this mode. Earlier results, however, indicated similar behavior for the fragmentation of thermometer ions; i.e., compared to the pulsating mode, softer ionization was achieved in the cone-jet regime.<sup>65</sup> To further investigate this relationship, we compared the mass spectra of myoglobin electrosprayed from unbuffered and buffered solutions

(75) Hughson, F. M.; Wright, P. E.; Baldwin, R. L. *Science* **1990**, *249*, 1544–1548.

(76) Griko, Y. V.; Privalov, P. L. *J. Mol. Biol.* **1994**, *235*, 1318–1325.

(77) Privalov, P. L. *J. Mol. Biol.* **1996**, *258*, 707–725.

(78) Dobo, A.; Kaltashov, I. A. *Anal. Chem.* **2001**, *73*, 4763–4773.

(79) Gilmanshin, R.; Gulotta, M.; Dyer, R. B.; Callender, R. H. *Biochemistry* **2001**, *40*, 5127–5136.

in the two axial regimes (see Figure 2 in the Supporting Information). These experiments revealed that the changes in the spraying mode mostly affected the dissociation of the complex. Consistent with the results obtained for thermometer ions, the protein complex was preserved to a better degree in the cone-jet mode. The CSDs of the apo and holo forms did not appreciably shift with the change in the spraying regime.

This suggested that the dissociation of the holomyoglobin occurred at least in part in the gas phase via collision-activated dissociation. The conformations of the holo- and apoproteins, however, were affected by the spraying mode-induced pH changes of the electrosprayed solutions in the unbuffered system. The higher survival yield of the noncovalent complex in the cone-jet mode could be explained in terms of the smaller droplet sizes produced by this regime. First, the larger droplets in the pulsating mode may produce increased background gas pressure in the interface due to the higher solvent load. This in turn could increase the efficiency of collision-activated dissociation. Second, the smaller droplets and consequently lower background pressure in the cone-jet mode could result in enhanced evaporative droplet cooling and in the stabilization of the complex.<sup>65</sup> Thus, the diminished fragmentation of thermometer ions and the higher survival yield of noncovalent complexes in cone-jet mode could both be the result of the small (submicrometer) droplets produced by this spraying regime.

## CONCLUSIONS

The widespread application of ESI-MS for probing the solution-phase structure of proteins and noncovalent complexes requires a fundamental understanding of the underlying processes. These include the formation and dynamics of the electrified meniscus, the emergence of the filament, its breakup into droplets, and ultimately the release of gas-phase ions. In order to minimize structural changes in the protein ions during ESI, one needs to establish the most appropriate spraying conditions.

Earlier studies considered the influence of a variety of experimental factors on the CSDs of proteins, including the potential distributions created by the ion optics, the ion source temperature, and the solvent fractionation and acidification during droplet evaporation. These variables were reported to affect the chemical composition of the electrosprayed solution or interfere with the steps of ion generation. Therefore, their control is required for proteins sensitive to such changes.

The purpose of the present study was to elucidate the effect of axial spraying regimes on the conformation and noncovalent complexation of proteins. Our results demonstrated that switching between the pulsating and the cone-jet modes was followed by conformational changes of the protein ions. These changes appeared to mainly stem from the electrochemical redox processes inherent to the electrospray source. As the operating mode switched from the pulsating to the cone-jet regime, higher spray current was produced that had to be balanced by enhanced oxidation at the metal–liquid interface. Generally, this resulted in the oxidation of water and consequently the generation of protons. Thus, the concentration of the electrochemically pro-

duced protons increased when the spray switched to the cone-jet mode and, conversely, decreased upon returning to the pulsating mode.

These variations in the pH at the emitter affected the higher-order structure of the model proteins. Therefore, in protein folding studies utilizing ESI-MS, stabilization of the pH (through a buffer) or the spraying mode is well advised. This latter can be achieved by regulating the spray voltage via an electronic feedback based on spray current measurements<sup>80</sup> or through an automated optoelectronic system.<sup>66</sup>

Although the amount of net charge on the Taylor cone is different in the two studied spraying modes, it is negligible compared to the total amount of hydrogen ions balanced by counterions available in the same volume. For example, we measured the net charge on a Taylor cone with 65- $\mu\text{m}$  anchoring diameter based on the oscillation frequency in pulsating mode to be  $z = \sim 3 \times 10^7$  elementary charges.<sup>81</sup> The number of hydrogen ions in the Taylor cone volume for a solution with pH 3.75 is  $N_{\text{H}^+} = \sim 2 \times 10^{10}$ . Thus, the solution conformation of the protein is determined by the vast majority of the hydrogen ions present in the solution together with its counterion. At pH 3.75 or lower, changes between spraying modes in the availability of net charge are negligible compared to the reservoir of charges in the solution.

The selection of the spraying mode depends on the properties of the produced ions. Although in the pulsating mode the chemical composition of the electrosprayed solution is preserved to a better degree, the low ionization efficiency achieved and the enhanced dissociation of the produced ions probably due to the elevated pressure in the sampler cone–skimmer region of the mass spectrometer might be undesirable. For example, the cone-jet mode appears to be more suitable for the ionization of fragile molecules or noncovalent complexes that are insensitive to the lower pH created by this regime. For solutions of low buffer capacity, pH or redox buffers can be introduced to help minimize the changes in their chemical composition due to the switching between spraying modes.

The demonstrated relationship between the spraying mode and ionization properties (ionization efficiency, protein conformation, and the integrity of noncovalent complexes) offers a novel tool for the structural studies of proteins. For example, by adjusting the spray voltage, one can trigger a change in the spraying mode and follow the evolution of the protein ion charge-state distribution. Although its applications are limited to proteins with two folding states, compared to mixing techniques used to produce pH perturbations, this approach offers a simpler experimental setup and a better defined start time for protein folding dynamics studies. Selecting the appropriate spraying mode can also be used to stabilize noncovalent complexes for the undistorted determination of their binding constants.

## ACKNOWLEDGMENT

This material is based upon work supported by the National Science Foundation under Grant 0719232 and by the Research Enhancement Funds of the George Washington University. Any opinions, findings, and conclusions or recommendations expressed in this material are those of the author(s) and do not necessarily reflect the views of the National Science Foundation.

(80) Marginean, I.; Kelly, R. T.; Page, J. S.; Tang, K.; Smith, R. D. *Anal. Chem.* **2007**, *79*, 8030–8036.

(81) Marginean, I.; Nemes, P.; Parvin, L.; Vertes, A. *Appl. Phys. Lett.* **2006**, *89*, 064104.

## **SUPPORTING INFORMATION AVAILABLE**

Figure 1 containing the ubiquitin charge-state distributions in the two spraying modes as a function of methanol concentration is available. Figure 2 shows the integrity and CSDs of the myoglobin complex for pulsating and cone-jet spraying modes in unbuffered and buffered solutions. This

material is available free of charge via the Internet at <http://pubs.acs.org>.

Received for review July 6, 2007. Accepted October 22, 2007.

AC0714359